Carbohydrate Polymers 88 (2012) 530–536

Contents lists available at SciVerse ScienceDirect

Carbohydrate Polymers

journal homepage: www.elsevier.com/locate/carbpol

Spectroscopic study of acetylated kraft pulp fibers

Carmen-Mihaela Popescu[a,*], Per Tomas Larsson[b], Nicolae Olaru[a], Cornelia Vasile[a]

[a] "Petru Poni" Institute of Macromolecular Chemistry of Romanian Academy, 41A Gr. Ghica Voda Alley, Ro.700487, Iasi, Romania
[b] Innventia AB, Box 5604, SE-114 86 Stockholm, Sweden

ARTICLE INFO

Article history:
Received 3 September 2011
Received in revised form
14 December 2011
Accepted 24 December 2011
Available online 18 January 2012

Keywords:
Cellulose acetylation
CP/MAS ^{13}C nuclear magnetic resonance
Fourier transform infrared spectroscopy
X-ray diffraction

ABSTRACT

The unbleached and bleached kraft pulp samples were partial acetylated by heterogenous acetylation method using acetic anhydride in the presence of sulfuric acid as a catalyst, to modify their physical properties. The overall degree of acetylation varied from 0 to 1.04 and 0.82 by changing the time of reaction up to 24 h. The characterization of acetylated kraft pulp samples, by solid-state CP/MAS ^{13}C nuclear magnetic resonance, Fourier transform infrared spectroscopy and X-ray diffraction, showed the formation of a heterogeneous structure. All three investigation methods give consistent results in qualitative terms.

The NMR results confirm the successful acetylation, indicating the regio-nonselective reactivity of the three kinds of OH groups. This may be due to the characteristic reaction that proceeds in a very thin layer between the acetylated and non-acetylated regions in each microfibril. The FT-IR data further provided a clear evidence for successful acetylation by decreasing of the bands assigned to the O—H stretching or deformation vibrations, and increasing of the bands assigned to the C═O and C—O in acetyl and carboxylic groups. Furthermore, as the acetylation reaction proceeds, was identified a new band at 3032 cm^{-1} assigned to the —CH_3 asymmetric stretching belonging to acetyl groups. The band from 2945 cm^{-1}, assigned to the >CH_2 asymmetric stretching, was shifted to higher wavenumbers and both bands increased in intensity with increasing acetylation time. These modifications occur because the hydroxyl groups from the anhydroglucose are partially substituted by acetyl groups in the reaction. X-ray diffraction profiles of the acetylated samples showed similar crystalline patterns with that of unmodified cellulose, but the changes of band widths and intensities indicated that acetylation proceeded from the surface of microfibrils towards the core of each microfibril.

1. Introduction

Cellulose is the most abundant and renewable biopolymer in nature, biosynthesized in the cell wall of higher plants, bacteria, algae, and some fungi. It is an optically anisotropic polysaccharide made up of poly-(1→4)-β-D-glucose chains. Due to the numerous strong polar groups, cellulose molecules are linked by hydrogen bonds within the molecule and between different molecules. Crystallographic studies showed that the secondary structure of native cellulose is a ribbon-like conformation with an approximately twofold helical structure. As generally known and accepted, the hydrogen bonds play an important role in the conformational and mechanical properties of the cellulosic materials (He, Tang, & Wang, 2008).

Cellulose acetate is one of the most important cellulose derivatives, being used in application such as: membranes, films, fibers, plastics, filters, and so on (Yang, Xu, Ma, & Wang, 2008).

Cellulose acetates are produced according to two distinct methodologies, which are referred to as homogeneous and heterogeneous processes from different cellulose sources such as: cotton, sugar cane bagasse, wood and others (Rodrigues Filho et al., 2000). In the homogeneous process, cellulose is acetylated by a solution containing acetic acid, acetic anhydride and a catalyst, usually sulfuric acid, and the produced cellulose acetate is solubilized in the reaction medium. In the heterogeneous process, a non swelling diluent is added to the system, which causes the produced cellulose acetate to remain insoluble.

Few studies have reported on the production of cellulose acetates via bacterial cellulose acetylation (Barud et al., 2008; Yamamoto, Horii, & Hirai, 2006).

The acetylation process depends on the accessibility of cellulose fibers and the susceptibility of individual cellulose I surfaces. Cellulose acetate is obtained from cellulose through the substitution of its cellulosic hydroxyl groups by acetyl groups. The properties of cellulose acetate depend on its degree of substitution, i.e. the average number of acetyl groups per anhydroglucose unit, and on the substituent distribution at three possible sites of anhydroglucose unit and along the length of cellulose chain (He et al., 2008).

* Corresponding author. Tel.: +40 232 217454; fax: +40 232 211299.
E-mail address: mihapop@icmpp.ro (C.-M. Popescu).

0144-8617/$ – see front matter © 2012 Elsevier Ltd. All rights reserved.
doi:10.1016/j.carbpol.2011.12.046

The control of the acetylation time can be an important aspect to the variable degree of acetylation and cellulose acetate's physical structure (Barud et al., 2008).

The fibrous conversion method also provides partially acetylated cellulosic materials. Herdle and Griggs (1965) prepared a paper with improved wet strength and dimensional stability from partially acetylated cellulose fibers. Sassi, Tekely, and Chanzy (2000) studied the homogeneous acetylation process for Valonia and tunicate cellulose samples at the initial undissolved stage by CP/MAS ^{13}C NMR, FT-IR and electron microscopy. As a result, it was found that acetylation proceeds from the surface to the core of each microfibril and the I_α crystals undergo acetylation more rapidly than the I_β crystals.

Since the acetylated surface is expected to provide improved adhesion with hydrophobic matrices, use of partial acetylation of cellulosic fibers has been intensively studied as reinforcing elements for composite materials (Kim, Nishiyama, & Kuga, 2002; Matsumura & Glasser, 2000).

In this paper, cellulose acetates were produced from unbleached and bleached kraft pulp fibers using heterogenous acetylation under acetic anhydride medium, without solvents and in the presence of sulfuric acid catalyst. The chemical modifications were observed as a function of acetylation time and characterized by solid state CP/MAS ^{13}C nuclear magnetic resonance (NMR), Fourier transform infrared spectroscopy (FTIR) and X-ray diffraction.

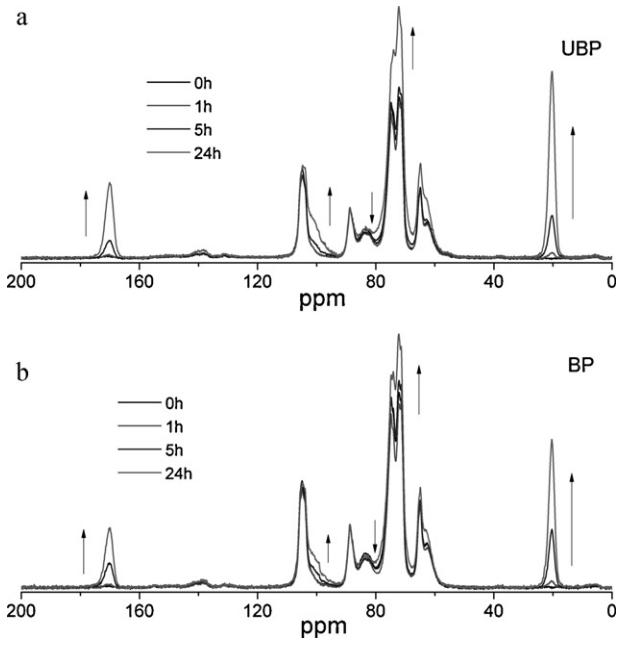

Fig. 1. CP/MAS ^{13}C NMR spectra of non-acetylated and acetylated unbleached (UBP) (a) and bleached (BP) (b) kraft pulp samples.

2. Materials and methods

2.1. Materials

Bleached (BP) and unbleached (UBP) mixed spruce and pine kraft pulp fibers samples from Södra Cell, Sweden (courtesy Karin Sjöström) were wet-defibrated and air-dried at room temperature several days then oven-dried at 80 °C for 24 h. 1.5 g of each sample were suspended in a mixture of 7.5 mL acetic anhydride and 0.015 mL sulfuric acid (as a catalyst), and vigorously stirred. Acetylation was performed at 30 °C for different reaction times: 1, 5 and 24 h. After the desired reaction time, samples were separated from suspension by filtration, then washed several times with distilled water, and air-dried at room temperature.

2.2. Methods

Solid-state CP/MAS ^{13}C NMR spectroscopy. High-resolution solid state ^{13}C NMR spectra were recorded at 7.04 *T* with cross-polarization/magic angle spinning (CP/MAS) in a Bruker Avance AQS 300 WB spectrometer. All powdered samples were packed uniformly in a zirconium oxide rotor. All measurements were performed at 289 ± 1 K. The MAS rate was 5 kHz. A double air-bearing probe was used. Acquisition was performed with a CP pulse sequence, using a 4.5 μs proton 90° pulse, 800 μs ramped (100–50%) falling contact pulse and a 2.5 s delay between repetitions. A TPPM15 pulse sequence was used for ^{1}H decoupling. Glycine was used for Hartman–Hahn matching procedure and as external standard for the calibration of the chemical shift scale relative to tetramethylsilane ($(CH_3)_4Si$). The data point of maximum intensity in glycine carbonyl line was assigned a chemical shift of 176.03 ppm.

FT-IR spectra were recorded on solid samples in KBr pellets by means of FT-IR DIGILAB ScimitarSeries spectrometer with a resolution of 4 cm^{-1}. The concentration of the sample in the tablets was constant – of 5 mg/500 mg KBr. Five recordings were performed for each sample after successive milling and the evaluations were made on the average spectrum obtained from these five recordings. Processing of the spectra was done by means of Grams/32 program (Galactic Industry Corporation).

The *X-ray diffraction (XRD)* analysis was performed on a Bruker AD8 ADVANCE Wide Angle Xray Diffraction. Bragg–Brentano parafocusing goniometer, scans recorded in step mode by using the Ni-filtered Cu Kα radiation (λ = 0.1541 nm). The working conditions were 36 kV and 30 mA tube power. All the diffractograms were collected in the range of 2–40 2θ degrees, at room temperature. The recorded diffractograms were deconvoluted using Gaussian profiles by means of Grams/32 program (Galactic Industry Corp.). The reduced chi-squared value, for all deconvoluted curves was $\chi^2 \leq 0.1$. After deconvolution, several parameters can be calculated and compared, e.g. the crystalline index, the apparent crystallite size, and the proportion of crystallite interior chains.

3. Results and discussions

3.1. Solid-state CP/MAS ^{13}C NMR spectroscopy

Natural cellulose fibers have a molecular architecture with a high degree of individuality, depending on their biological origin. Typical CP/MAS ^{13}C NMR spectra from cellulose I are made up of six signals from the anhydroglucose unit split into fine structure of the cellulose I fibril. The information in this fine structure is high, but the accessibility of the information is hampered by a severe overlap of the signals (Larsson, Wickholm, & Iversen, 1997; Wickholm, Larsson, & Iversen, 1998).

The successful acetylation of unbleached (UBP) and bleached (BP) pulp samples was confirmed by CP/MAS ^{13}C NMR spectra. The spectra of non-acetylated and acetylated samples showed characteristic signals (Fig. 1 summarized in Table 1). For evaluation, the spectra were normalized to the band at 88.7 ppm assigned to crystalline C4.

The assignments were made in accordance with literature (Larsson, Hult, Wickholm, Pettersson, & Iversen, 1999; Larsson et al., 1997; Wickholm et al., 1998).

The spectra for acetylated samples showed a set of signals that confirms modification in the unbleached and bleached pulp structure. The respective signals for cellulose acetate are assigned

Table 1
Resonance assignments of CP/MAS ^{13}C NMR signals of kraft pulp samples.

Chemical shift (ppm)	Assignment
171.4	*COO— in acetyl groups*
104.8	C-1 in cellulose Iα, Iβ and less-ordered cellulose
101.4	*C-1 in the cellulose acetate*
88.7	C-4 in crystalline cellulose Iα, Iβ and paracrystalline cellulose
83.7	C-4 in non-crystalline cellulose or less ordered surface cellulose molecules
74.8	C-2,-3,-5 in cellulose and hemicelluloses
72.1	C-2,-3,-5 in cellulose and hemicelluloses
71.4	C-2,-3,-5 in cellulose and hemicelluloses
64.8	C-6 in crystalline cellulose Iα, Iβ and paracrystalline cellulose
62.6	C-6 in non-crystalline cellulose or less ordered surface cellulose molecules
20.6	*CH_3— in acetyl groups*

Italic for bands observed in the spectra after acetylation.

to the COO— (171.4 ppm), C1 (101.4 ppm), and CH_3 (20.6 ppm) (Yamamoto et al., 2006).

The crystalline and disordered components were detected for the C4 and C6 carbon, respectively (Yamamoto et al., 2006). The intensity of the signal 64.8 ppm for crystalline C6, decreased and the amorphous background increased with increasing reaction time. These reveal the crystalline structure of the cellulose was disrupted and the acetylation reaction occurs in the system. Finally, the increase of the intensity for COO— and CH_3— indicated that the extent of acetylation increased during reaction period.

These changes are observed due to microfibrils modifications after acetylation, being obtained a product less crystalline than unmodified cellulose. In addition, the ordered components of cellulose have been found to decrease at almost the same rate with the increase of reaction time. This indicates that the OH groups associated with these carbons undergo acetylation almost simultaneously, independently on the position in the anhydroglucose units and in structure between the ordered and disordered OH groups. This may be due to the three OH groups underwent acetylation at nearly the same time in a very thin layer produced at the boundary between the acetylated and non-acetylated regions and successively move from the surface to the inner part in each nanofibril (Hu, Chen, Xu, & Wang, 2011; Yamamoto et al., 2006). Similar regio-nonselective reactivity of the OH groups in the anhydroglucose units was also observed for acetylation of cellulose by Sassi et al. (2000).

The acetylation gradually modified the NMR spectra patterns. These modifications are associated to three factors: changes in the acetylation degree during the synthesis, the low homogeneity in the distribution of substitution groups and the crystalline structure.

The same acetylation effect was observed in both types of unbleached and bleached pulps. However, differences in signal intensities were stronger for unbeached pulp than for bleached one. This means that the acetylation was more pronounced in the case of the unbleached pulp sample. After integration of the regions between 30 and 11 ppm, assigned to CH_3 from acetyl groups, and 115 and 50 ppm, assigned to C1–6 carbons from cellulose, it was possible to evaluate the bulk acetylation degree (Fig. 2).

Thus, after 5 h the bulk acetylation degree was slightly lower for unbleached pulp (0.34 and 0.39) while it was clearly higher after 24 h, as compared with the bleached pulp, of 1.08 in respect with 0.82. This can be explained by an increased number of OH groups (due to the presence of hemicelluloses and lignin) and a less ordered structure of the unbleached pulp than bleached one, so being more susceptible to attack of reagent (acetylation).

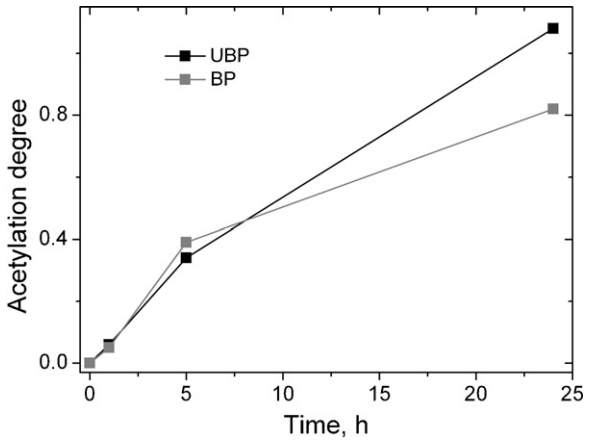

Fig. 2. Bulk acetylation degree versus reaction time of unbleached (UBP) and bleached (BP) kraft pulp samples.

3.2. FT-IR spectroscopy

Fourier transform infrared spectroscopy (FT-IR) is a well-known powerful analytical tool to detect functional groups by measuring fundamental molecular vibrations. Especially carbonyl groups (of the ester groups) that have a high molar absorptivity can easily be seen, even at low concentrations. Therefore, many researchers characterizing and following the acetylation of wood have used this tool (Barud et al., 2008; Fan, Liu, Liu, & Lu, 2010; Hu et al., 2011; Yang et al., 2008).

The FT-IR spectra of untreated and acetylated unbleached and bleached kraft pulp samples in the range 4000–840 cm^{-1} are shown in Figs. 3 and 4 and all the major infrared absorption bands observed in the spectra are listed in Tables 2 and 3. The characteristic bands for unbleached and bleached kraft pulps and those associated to acetylated samples were identified and were assigned according to literature data (He, Zhang, Cui, & Wang, 2009; Hu et al., 2011; Jebrane, Pichavant, & Sebe, 2011; Nishiyama, Sugiyama, Chanzy, &

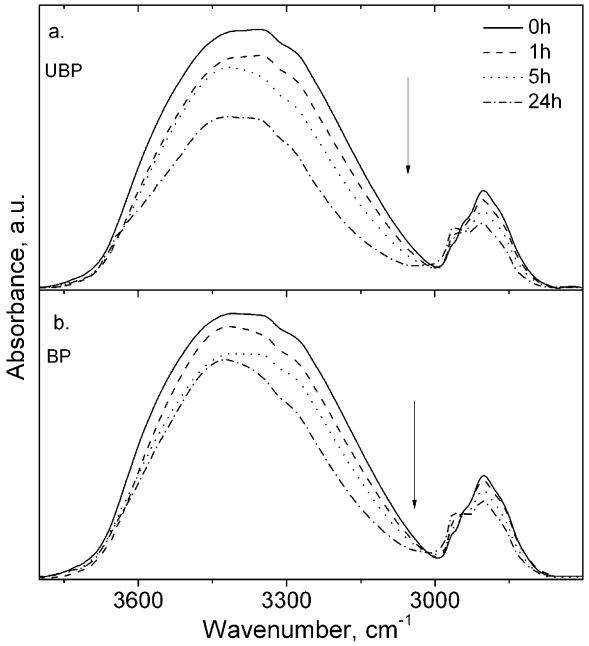

Fig. 3. FT-IR spectra in the 3800–2700 cm^{-1} of non-acetylated and acetylated unbleached (UBP) (a) and bleached (BP) (b) pulp samples.

Table 2
The characteristic bands in FT-IR spectra of the non-acetylated and acetylated kraft pulp samples in the 3800–2700 cm^{-1} region.

Band assignment	Wavenumber (cm^{-1})
Absorbed water weakly bound and intramolecular hydrogen bond in a phenolic group (in lignin)	3566
Multiple formation of an intermolecular hydrogen bond between phenolic groups and their combinations with alcoholic groups	3471
O2—H2···O6 intramolecular stretching modes (in cellulose)	3428
O3—H3···O5 intramolecular in cellulose	3342
O6—H6···O3 intermolecular in cellulose I_β (3270)	3273
O6—H6···O3 intermolecular in cellulose I_α (3240)	3222
—CH_3 asymmetric stretching	*3032*
>CH_2 asymmetric stretching	2945/*2962*
—CH_3 symmetric stretching	2903
>CH_2 symmetric stretching	2861

Italic for bands observed in the spectra after acetylation.

Langan, 2003; Perez & Mazeau, 2005; Popescu et al., 2007; Popescu et al., 2008).

3.2.1. The 3800–2700 cm^{-1} region

In this region, strong hydrogen bonded (O—H) stretching absorptions and prominent C—H stretching absorptions were observed (Fig. 3). The hydroxyl stretching region of the spectrum is particularly useful for elucidating hydrogen-bonding patterns because, each distinct hydroxyl group gives a single stretching band at a frequency that decreases with increasing strength of hydrogen bonding.

A broad band with a maximum around 3420 cm^{-1} was observed in the spectra of the kraft pulp samples. This band is an envelope of a series of bands which can be assigned to different hydrogen bonds (see Table 2). The intensity of this band decreases more pronounced in the spectra of the unbleached kraft pulp than in the spectra of bleached kraft pulp. The lowering of intensities of OH stretching band is consistent with the partial acetylation of the samples.

An intramolecular hydrogen bond vibration, derived from O2—H2···O6, is observed at 3428 cm^{-1}. This band shows a variation of the maximum with a few wavenumbers to higher values in the spectra of acetylated pulp samples. The band at 3271 cm^{-1} (assigned to the O6—H6···O3 intramolecular hydrogen bonds existing only in monoclinic Iβ phase) is shifted to higher wavenumbers with maximum 10 cm^{-1} after the acetylation process.

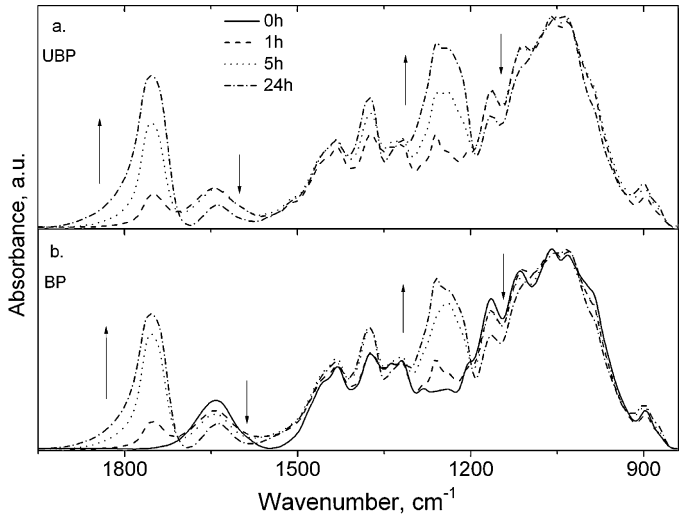

Fig. 4. FT-IR spectra in the 1900–850 cm^{-1} of non-acetylated and acetylated unbleached (UBP) (a) and bleached (BP) (b) pulp samples.

Table 3
The characteristic bands in FT-IR spectra of the non-acetylated and acetylated kraft pulp samples in the 1900–850 cm^{-1} region.

Band assignment	Wavenumber (cm^{-1})
Carbonyl C=O stretching of ester, unconjugated ketones, carbonyls groups	*1745*
Absorbed O—H and conjugated C—O	1642
C=C of aromatic skeletal (lignin)	1513
C—H deformation in lignin and carbohydrates, O—H in plane bending of cellulose	1461
C—H deformation in lignin and carbohydrates, O—H in plane bending of cellulose	1429
C—H deformation in cellulose and hemicelluloses, C—H bond in —O(C=O)—CH_3 group	1375
O—H in-plane bending	1339
O—H deformation and CH_2 rocking vibration	1317
C—H deformation	1281
C=O stretching	1262
C—O stretching in acetyl group	*1237*
O—H in-plane bending	1206
C—O—C asymmetric vibration	1166
C—O stretching vibration	*1127*
C—OH stretching vibration	1114
C—O—C deformation	*1082*
C—O stretching mainly from C(3)—O(3)H in cellulose	1060
C—O stretching ring in cellulose and hemicelluloses	1031
C—O stretching vibration	985
β-glucosidic linkage between the sugar units in hemicelluloses and celluloses	896

Italic for bands observed in the spectra after acetylation.

As the acetylation reaction proceed, a new band at 3032 cm^{-1} assigned to the —CH_3 asymmetric stretching was identified, being observed, in the same time, a shifting of the band at 2945 cm^{-1} (assigned to the >CH_2 asymmetric stretching) to higher wavenumbers with maximum 17 cm^{-1}. Both bands increased in intensity with increasing time of acetylation.

These modifications occur because the hydroxyl groups from the anhydroglucose are partially substituted by acetyl groups during the reaction.

3.2.2. The 1900–850 cm^{-1} region

The "fingerprint" region of the spectra of the non-acetylated and acetylated kraft pulps shows clear differences (Fig. 4). By comparing the spectral characteristics of both types of samples, differences in their chemistry become clear and the spectral contributions of the different characteristic groups, as well as the band assignments can be ascertained (Table 3).

In addition, there are many well-defined peaks in the "fingerprint" region between 1900 and 850 cm^{-1} (Fig. 4). This region corresponds to different stretching, deformation, bending or rocking vibrations for principal groups from non-acetylated and acetylated kraft pulp samples. Thus, the evidence of acetylation is again clearly provided by the presence of and/or concentration increase of the important ester bonds at 1745 cm^{-1} assigned to carbonyl C=O stretching of ester, unconjugated ketones, carbonyls groups, 1375 cm^{-1} assigned to C—H bonds in —O(C=O)—CH_3 group, 1262 cm^{-1} assigned to C=O stretching and 1234 cm^{-1} assigned to C—O stretching of acetyl group in the spectra of the acetylated kraft pulp samples (see Table 3).

The absence of a peak at 1700 cm^{-1} for a carboxylic group in the spectra of the acetylated products also indicates that the samples do not contain acetic acid.

Apart from the important bands which appeared or increased in intensity with increasing reaction time were observed two new bands at 1127 and 1082 cm^{-1} assigned to C—O stretching vibration and C—O—C deformation, respectively. These bands were identified

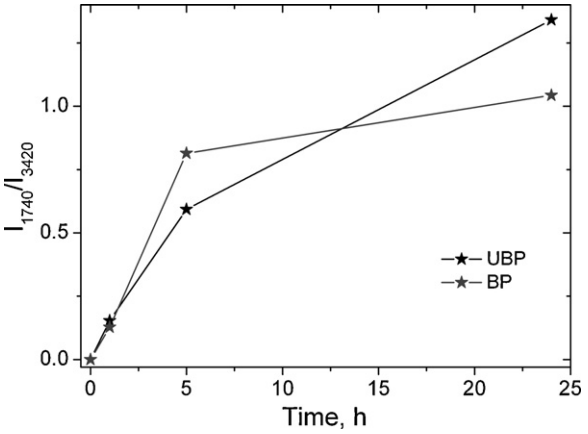

Fig. 5. Bulk acetylation degree against reaction time of unbleached (UBP) and bleached (BP) kraft pulp samples.

in the acetylated kraft pulp spectra, being observed to increase in intensity during the course of reaction.

In order to observe the level of acetylation of the kraft pulp samples, the extent of acetylation for all the samples was quantitatively determined by calculating the ratio between the intensity of the acetyl C=O stretching of ester at about 1740 cm^{-1} and the intensity of O—H stretching vibration at about 3420 cm^{-1} (I_{1740}/I_{3420}) (Fig. 5).

As in the case of bulk acetylation degree evaluated by CP/MAS ^{13}C NMR spectroscopy, after 5 h the acetylation degree has a lower value for unbleached kraft pulp while it has a higher value after 24 h as compared with the bleached kraft pulp. Due to well defined signals in the NMR spectra, compared to bands from IR spectra (which are an envelope of a series of individual bands), the more appropriate valued for the bulk acetylation degree are those obtained from NMR spectra. Even the bulk acetylation degree has values different; qualitatively it presents the same variation.

3.3. X-ray diffraction

To obtain further information, wide-angle X-ray diffractograms were also measured for the same acetylated samples, as shown in Fig. 6. The XRD results allow us to analyze changes in the crystallinity of the samples after the acetylation for different periods.

Reflections from the 15.0–15.2° 2θ (assigned to the (1 0 1) crystallographic plane), 16.7–16.8° 2θ (assigned to the (1 0 $\bar{1}$) crystallographic plane), 19.0° 2θ (assigned to amorphous phases), 20.0° 2θ (assigned to the (1 0 2) crystallographic plane), and 22.5° 2θ (assigned to the (0 0 2) or (2 0 0) crystallographic plane of cellulose I) are observed in both non-acetylated and acetylated samples (Fig. 7).

These observations are in accordance with the existence of the resonance lines and specific bands from NMR and IR spectra assigned to cellulose. Moreover, broad reflection at 8° 2θ, cited as the principal characteristic of semicrystalline acetylated derivative cellulose (Rodrigues Filho et al., 2000), is observed to appear after 5 h of acetylation. The position of this band indicates the generation of a disorder when kraft pulp was acetylated.

The crystallinity degree from X-ray diffractograms was calculated according to equation proposed by Hermans (Marcovich, Reboredo, & Aranguren, 2001):

$$\mathrm{CrI} = \frac{A_{\mathrm{crist}}}{A_{\mathrm{total}}} \quad (1)$$

where CrI is the crystallinity degree, A_{crist} is the sum of crystalline peak areas, and A_{total} is the total area under diffractogram.

The degree of crystallinity (CrI) is higher for bleached pulp (62.2%) sample than for unbleached (60.2%) one and decreases

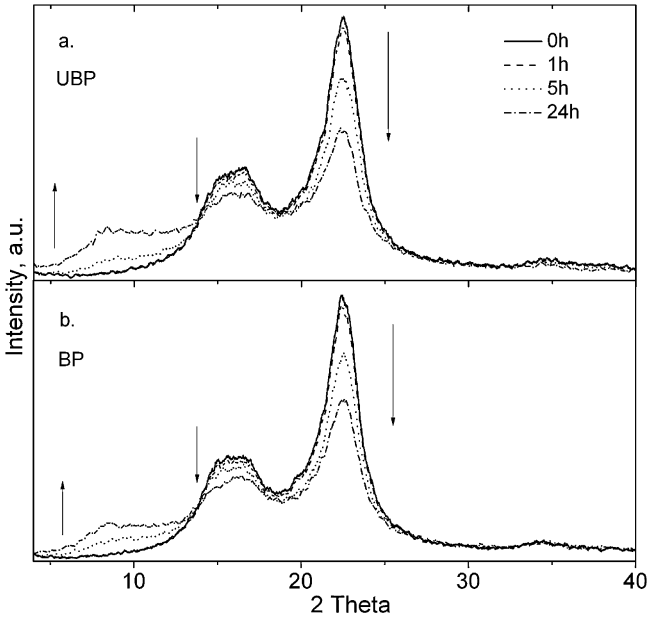

Fig. 6. X-ray diffractograms of non-acetylated and acetylated unbleached (UBP) (a) and bleached (BP) (b) kraft pulp samples.

with the increases time of reaction to 57.8% and 58.6%, respectively (Fig. 8).

Crystallinities of samples were estimated from FT-IR spectra using a method proposed by Hulleman, Van Hazendonk, and Vna Dam (1994). The ratio between the absorption intensities of the band at 1280 cm^{-1}, assigned to the C—H bending mode and at 1200 cm^{-1}, assigned to the C—O—C stretching mode of the pyranose ring ($R_{c,h} = I_{1280}/I_{1200}$) was used to determine cellulose crystallinity.

$$x_c = 1.06 \times R_{c,h} + 0.19 \quad (2)$$

This correlation is valid only in the range $0.26 \leq x_c \leq 0.75$, the cellulose crystallinity limits used by Hulleman et al. (1994). The values obtained were 61 ± 1% and 62 ± 1% for the untreated unbleached and the bleached pulps, respectively, and decreases to 58 ± 1% and 59 ± 1% for 24 h treated samples (Fig. 8). FT-IR determinations of the degree of crystallinity were in good agreement with those obtained by XRD measurements.

The acetylated kraft pulps present weaker diffraction bands from cellulose I than those in the untreated samples, and in consequence, a low degree of crystallinity compared with that of the original ones. This is due to the substitution of the hydroxyl groups

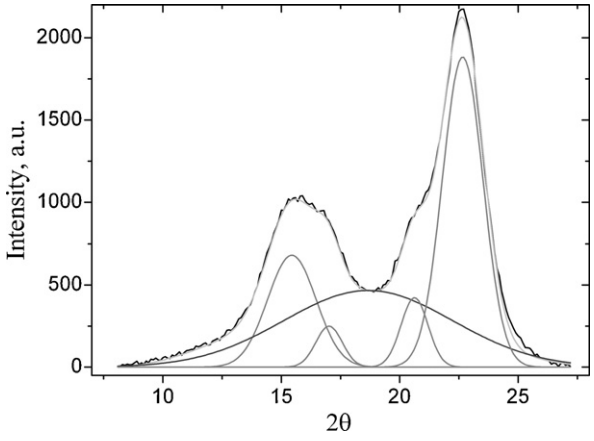

Fig. 7. Deconvoluted X-ray diffractograms of unbleached (UBP) kraft pulp fibers.

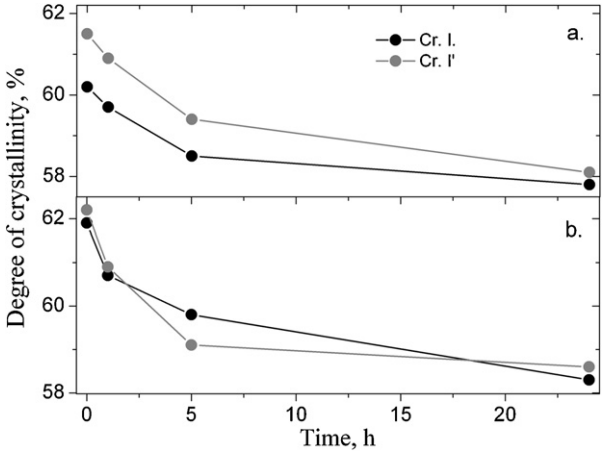

Fig. 8. Degree of crystallinity vs reaction time for unbleached (UBP) (a) and bleached (BP) (b) kraft pulp samples (CrI, crystallinity degree from XRD; Cr.I′, crystallinity degree from FT-IR spectroscopy).

by acetyl groups with greater volume, which broke the inter- and intra-molecular hydrogen bonds of cellulose.

These results may support the presumption that the present acetylation proceeds from the surface to the core of each microfibril with the increase of reaction time, and the crystal structure of the nanofibers changed with the increase of the acetylation degree, similar to the case in the previous report (Hu et al., 2011).

Apart from cellulose which is the major component of the kraft pulps fibers, other constituents include lignin and hemicelluloses (especially in the unbleached kraft pulp). Phenolic, benzylic or alcoholic (primary and secondary) hydroxyl groups are present in the lignin region while only the alcoholic hydroxyl groups are found in the carbohydrate. The different types of hydroxyl groups will therefore undergo different susceptibility towards acetylation. It has been previously reported by various workers (Adebajo & Frost, 2004; Hill, Jones, Strickland, & Cetin, 1998) that the initial step in the mechanism for the reaction of acetic anhydride with a hydroxyl group involves a nucleophilic attack on the acyl carbon centre of the acetic anhydride molecule by a pair of the alcoholic (or phenolic) hydroxyl group followed by subsequent loss of acetic acid to generate the ester. The rate of diffusion of acetic anhydride into the cell wall can also limit the rate of reaction for whole pulp fibers.

4. Conclusions

The three analytical methods confirmed the partial successful acetylation of the unbleached and bleached kraft pulp samples. The overall bulk degree of acetylation after 24 h of the acetylation reaction was of 1.04 for unbleached kraft pulp and of 0.82 for bleached one, respectively.

The NMR spectra for acetylated samples showed a set of signals that confirms modification in the unbleached and bleached kraft pulp structure. The intensity of the crystalline and disordered components for the C4 or C6 carbon decreased with increasing reaction time. These reveal that the crystalline structure of the cellulose was disrupted and the acetylation reaction occurs in the system. Finally, the increase of the intensity for COO— and CH_3— indicated that the extent of acetylation increased. The acetylation gradually modified the characteristic of the NMR spectra patterns. These modifications are associated to three factors: changes in the acetylation degree during the synthesis, the low homogeneity in the distribution of substitution groups and the crystalline structure.

From FT-IR spectra was clearly evidenced the decreasing of the bands assigned to the O—H stretching or deformation vibrations at 3420, 1337, 1310, 1206 and 1114 cm^{-1} and increasing of the bands assigned to the C=O and C—O in acetyl and carboxylic groups at 1745, 1375, 1262 and 1234 cm^{-1}. Furthermore, as the acetylation reaction proceed, was identified a new band at 3032 cm^{-1} assigned to the —CH_3 asymmetric stretching. In the same time was observed the shifting of the band from 2945 cm^{-1}, assigned to the >CH_2 asymmetric stretching, to higher wavenumbers with maximum 17 cm^{-1}. Both bands increased in intensity with increasing time of acetylation. These modifications occur because the hydroxyl groups from the anhydroglucose are partially substituted by acetyl groups in the reaction.

X-ray diffraction profiles of the acetylated samples showed the crystalline pattern of unmodified cellulose, but with changes in bands widths and intensity. Moreover, a broad reflection at 8° 2θ, cited as the principal characteristic of semicrystalline acetylated derivative cellulose was identified in acetylated samples more than 5 h. The acetylated kraft pulps present smaller diffraction bands from cellulose I than those in the untreated samples, and in consequence, a low degree of crystallinity compared with that of the original ones. This is due to the substitution of the hydroxyl groups by acetyl groups with greater volume, which broke the inter- and intra-molecular hydrogen bonds of cellulose.

Acknowledgments

The EU COST Action E54 “Characterization of the fine structure and properties of papermaking fibers using new technologies” is acknowledged for financial support.

References

Adebajo, M. O., & Frost, R. L. (2004). Acetylation of raw cotton for oil spill cleanup application: An FTIR and ^{13}C MAS NMR spectroscopic investigation. *Spectrochimica Acta A*, *60*, 2315–2321.

Barud, H. S., de Araujo Junior, A. M., Santos, D. B., de Assuncao, R. M. N., Meireles, C. S., Cerqueira, D. A., et al. (2008). Thermal behavior of cellulose acetate produced from homogeneous acetylation of bacterial cellulose. *Thermochimica Acta*, *471*, 61–69.

Fan, X.-S., Liu, Z.-T., Liu, Z.-W., & Lu, J. (2010). Cellulose acetate membrane synthesis from biomass of ramie. *Journal of Applied Polymer Science*, *117*, 588–595.

He, J., Tang, Y., & Wang, S.-Y. (2008). Alkaline treatment of diacetate fibers and subsequent cellulase degradation. *Journal of Applied Polymer Science*, *107*, 2466–2474.

He, J., Zhang, M., Cui, S., & Wang, S.-Y. (2009). High-quality cellulose triacetate prepared from bamboo dissolving pulp. *Journal of Applied Polymer Science*, *113*, 456–465.

Herdle, L. E., & Griggs, W. H. (1965). Partially acetylated cellulose—its properties and potential applications. *Tappi*, *48*, 103–107.

Hill, C. A. S., Jones, D., Strickland, G., & Cetin, N. S. (1998). Kinetic and mechanistic aspects of the acetylation of wood with acetic anhydride. *Holzforschung*, *52*, 623–629.

Hu, W., Chen, S., Xu, Q., & Wang, H. (2011). Solvent-free acetylation of bacterial cellulose under moderate conditions. *Carbohydrate Polymers*, *83*, 1575–1581.

Hulleman, S. H. D., Van Hazendonk, J. M., & Vna Dam, J. E. G. (1994). Determination of crystallinity in native cellulose from higher plants with diffuse reflectance Fourier transform infrared spectroscopy. *Carbohydrate Research*, *261*, 163–172.

Jebrane, M., Pichavant, F., & Sebe, G. (2011). A comparative study on the acetylation of wood by reaction with vinyl acetate and acetic anhydride. *Carbohydrate Polymers*, *83*, 339–345.

Kim, D.-Y., Nishiyama, Y., & Kuga, S. (2002). Surface acetylation of bacterial cellulose. *Cellulose*, *9*, 361–367.

Larsson, P. T., Hult, E. L., Wickholm, K., Pettersson, E., & Iversen, T. (1999). CP/MAS ^{13}C NMR spectroscopy applied to structure and interaction studies on cellulose I. *Solid State NMR*, *15*, 31–40.

Larsson, P. T., Wickholm, K., & Iversen, T. (1997). A CP/MAS ^{13}C NMR investigation of molecular ordering in celluloses. *Carbohydrate Research*, *302*, 19–25.

Marcovich, N. E., Reboredo, M. M., & Aranguren, M. I. (2001). Modified woodflour as thermoset fillers. II. Thermal degradation of woodflours and composites. *Thermochimica Acta*, *372*, 45–57.

Matsumura, H., & Glasser, W. G. (2000). Cellulosic nanocomposites. II. Studies by atomic force microscopy. *Journal of Applied Polymer Science*, *78*, 2254–2261.

Nishiyama, Y., Sugiyama, J., Chanzy, H., & Langan, P. (2003). Crystal structure and hydrogen bonding system in cellulose Iα from synchrotron X-ray and neutron fiber diffraction. *Journal of American Chemical Society*, *125*, 14300–14306.

Perez, S., & Mazeau, K. (2005). Conformations, structures, and morphologies of celluloses. In S. Dumitriu (Ed.), *Polysaccharides II—Structural diversity and functional versatility* (pp. 41–68). New York: Marcel Dekker.

Popescu, C.-M., Popescu, M.-C., Singurel, Gh., Vasile, C., Argyropoulos, D. S., & Willför, S. (2007). Spectral characterization of Eucalyptus wood. *Applied Spectroscopy*, *61*, 1168–1177.

Popescu, C.-M., Tibirna, C. M., Raschip, I. E., Popescu, M.-C., Ander, P., & Vasile, C. (2008). Bulk and surface characterization of unbleached and bleached softwood kraft pulp fibres. *Cellulose Chemistry and Technology*, *42*(9–10), 525–547.

Rodrigues Filho, G., da Cruz, S. F., Pasquini, D., Cerqueira, D. A., Prado, V. S., & Assuncao, R. M. N. (2000). Water flux through cellulose triacetate films produced from heterogeneous acetylation of sugar cane bagasse. *Journal of Membrane Science*, *177*, 225–231.

Sassi, J.-F., Tekely, P., & Chanzy, H. (2000). Relative susceptibility of the Ia and Ib phase of cellulose towards acetylation. *Cellulose*, *7*, 119–132.

Wickholm, K., Larsson, P. T., & Iversen, T. (1998). Assignment of non-crystalline forms in cellulose I by CP/MAS ^{13}C NMR spectroscopy. *Carbohydrate Research*, *312*, 123–129.

Yamamoto, H., Horii, F., & Hirai, A. (2006). Structural studies of bacterial cellulose through the solid-phase nitration and acetylation by CP/MAS ^{13}C NMR spectroscopy. *Cellulose*, *13*, 327–342.

Yang, Z., Xu, S., Ma, X., & Wang, S. (2008). Characterization and acetylation behavior of bamboo pulp. *Wood Science and Technology*, *42*, 621–632.